Anisotropic Non-Stationary Image Estimation and its Applications: Part I. Restoration of Noisy Images

Hans Knutsson, Roland Wilson and Gösta H. Granlund

Hans Knutsson, Roland Wilson and Gösta H. Granlund, Anisotropic Non-Stationary Image Estimation and its Applications: Part I. Restoration of Noisy Images, 1983, IEEE Transactions on Communications, (COM--31), 3, 388-397.
http://dx.doi.org/10.1109/TCOM.1983.1095832

Anisotropic Nonstationary Image Estimation and Its Applications: Part I—Restoration of Noisy Images

HANS E. KNUTSSON, ROLAND WILSON, AND GOESTA H. GRANLUND, MEMBER, IEEE

Abstract—**A new form of image estimator, which takes account of linear features, is derived using a signal equivalent formulation. The estimator is shown to be a nonstationary linear combination of three stationary estimators. The relation of the estimator to human visual physiology is discussed. A method for estimating the nonstationary control information is described and shown to be effective when the estimation is made from noisy data. A suboptimal approach which is computationally less demanding is presented and used in the restoration of a variety of images corrupted by additive white noise. The results show that the method can improve the quality of noisy images even when the signal-to-noise ratio is very low.**

I. INTRODUCTION

THE estimation of images is a fundamental problem which lies at the heart of two related areas of image processing: restoration and coding.

The restoration problem is essentially one of optimal filtering with respect to some error criterion. The most tractable criterion—mean squared error—has formed the basis for most of the published work in the area [1]-[3]. The classical stationary solution to the problem, the Wiener filter, has been used with limited success because of its low-pass character, which gives rise to unacceptable blurring of lines and edges in the scene. Recently, a number of attempts to overcome this problem have adopted a nonstationary approach, which exploits the lower noise visibility in the vicinity of edges [4], [5] (the so-called "masking effect"). Unfortunately, the resulting filter structures are often rather cumbersome, requiring solution of the optimization equation at each point in the image.

A new approach with considerable appeal, because of its simplicity, is that of Abramatic and Silverman [6]. By expressing the masking effect in terms of the signal to be estimated, they were able to represent the nonstationary filter as a linear combination of two stationary filters, one of which was simply the identity mapping (i.e., a δ-function). Using a similar approach, but one derived primarily from consideration of the physiological properties of the human visual system, the authors of the present paper obtained satisfactory results in the enhancement of noisy images [7].

Over the same period of time, the development of predictive image coding methods has seen a similar shift from stationary DPCM systems [8], [9] to more complex, nonstationary and hybrid systems [10]-[14]. It is clear that a similar motivation to that described above lies behind this trend: the recognition that lines and edges constitute a substantive nonstationarity in the image model, that they introduce local anisotropy, and that, above all, they are significant to the human viewer. That this should be so is not surprising when one considers the importance attached to edge and line detection in image analysis and pattern recognition [17]-[19]. Such a view is strengthened by the accumulation of psychophysical and physiological data confirming linear feature detection as a primary function of the lower levels of the visual system [20]-[34]. A study of these aspects of the problem led Granlund to propose a "general-operator" theory for image processing [19]. The principles outlined by Granlund—the importance of locally "linear" features and of directionality in images—underlie several recent papers on image analysis [35], [36] as well as the work described in [7] and below. Moreover, a processor based on the "general operator" principle [37] has been the vehicle for all of the experimental work described herein.

This paper contains a generalization of the results of [7] into a nonstationary, anisotropic solution to the image estimation problem. Its relation to the work of Abramatic and Silverman and to human visual physiology will be discussed. A suboptimal approach will be presented and the results of experiments in image restoration will be discussed. In the concluding section, the general applicability of the method and its possible extensions will be considered. In the accompanying paper, a solution to the related problem of predictive coding is described.

II. NONSTATIONARY ESTIMATION AND ITS RELATION TO THE VISUAL SYSTEM

The most general statement of the estimation problem is: given a set of data $g(x, y)$, find the estimate $\hat{f}(x, y)$ of an image $f(x, y)$ which minimizes some distance $\|f(x, y) - \hat{f}(x, y)\|$ between original and estimate. The most commonly used distance is mean squared error. It is then possible to derive the estimate by using the orthogonality principle [38]

$$E\{[f(x, y) - \hat{f}(x, y)]g(x', y')\} = 0. \tag{1}$$

In terms of the correlation functions $R_{fg}(\cdot, \cdot, \cdot, \cdot)$ and $R_{\hat{f}g}(\cdot,$

Paper approved by the Editor for Signal Processing and Communication Electronics of the IEEE Communications Society for publication without oral presentation. Manuscript received August 7, 1981; revised May 18, 1982. This work was supported by the Swedish National Board for Technical Development and by SERC of the United Kingdom.

H. E. Knutsson and G. H. Granlund are with the Picture Processing Laboratory, Linkoeping University, S-581 83 Linkoeping, Sweden.

R. Wilson is with the Department of Electrical and Electronic Engineering, University of Aston, Birmingham B4 7PB, England, on leave at the Picture Processing Laboratory, Linkoeping University, S-581 83 Linkoeping, Sweden.

0090-6778/83/0300-0388$01.00

$\cdot, \cdot, \cdot)$, (1) can be expressed as

$$R_{fg}(x, x', y, y') = R_{\hat{f}g}(x, x', y, y'). \tag{2}$$

In the classical case of linear, stationary estimation, $\hat{f}(\cdot, \cdot)$ can be written as

$$\hat{f}(x, y) = h(x, y) * g(x, y) = \int_{-\infty}^{\infty} \int_{-\infty}^{\infty} h(\sigma, \nu) g(x - \sigma, y - \nu)\, d\sigma\, d\nu \tag{3}$$

giving for (1)

$$R_{fg}(x, y) = h(x, y) * R_{gg}(x, y). \tag{4}$$

In the case of restoration, a noncausal model of the image is permitted, while in prediction, it is necessary to specify a time direction. It will be assumed that the y-coordinate represents the vertical direction and that, in prediction, only lines above the current line are available. Thus, $h(x, y) = 0, y \leq 0$, for the predictor and in that case (4) is satisfied only for $y > 0$. In the unconstrained case, (4) may be expressed in terms of the power spectra, giving the familiar Wiener filter

$$H(w_1, w_2) = \frac{S_{fg}(w_1, w_2)}{S_{gg}(w_1, w_2)}. \tag{5}$$

A similar derivation, via the Wiener-Hopf equation [38], is possible for the predictor.

When the data is the sum of the image and stationary white noise of variance σ_n^2

$$g(x, y) = f(x, y) + n(x, y) \tag{6}$$

$$R_{nn}(x, y) = \sigma_n^2 \delta(x) \delta(y)$$

the Wiener solution becomes

$$H(w_1, w_2) = \frac{S_{ff}(w_1, w_2)}{S_{ff}(w_1, w_2) + \sigma_n^2}. \tag{7}$$

The modification made to this solution is the introduction of a visibility function $\alpha(x, y), 0 \leq \alpha(x, y) \leq 1$, which depends on the magnitude of the luminance gradient [6]. Having chosen the function $\alpha(\cdot, \cdot)$, the key issue remains of determining how it should affect the estimation. Abramatic and Silverman showed that the "generalized Backus and Gilbert" criterion yields a solution

$$H'(w_1, w_2) = \frac{S_{ff}(w_1, w_2)}{S_{ff}(w_1, w_2) + \alpha(x, y)\sigma_n^2}. \tag{8}$$

This approach has the undesirable feature that the filter changes from point to point in a way which is generally burdensome computationally. They proposed a "signal equivalent" approach, defining a modified signal

$$f_1(x' - x, y' - y) = \alpha(x, y) f(x' - x, y' - y) + [1 - \alpha(x, y)] g(x' - x, y' - y) \tag{9}$$

yielding a filter $H_1(\cdot, \cdot, \cdot, \cdot)$

$$H_1(w_1, w_2, x, y) = \alpha(x, y) \frac{S_{ff}(w_1, w_2)}{S_{ff}(w_1, w_2) + \sigma_n^2} + [1 - \alpha(x, y)]. \tag{10}$$

This solution has the advantage that the modified filter is simply a linear combination of the stationary Wiener filter and the identity mapping

$$h_1(x', x, y', y) = \alpha(x, y) h(x' - x, y' - y) + [1 - \alpha(x, y)] \delta(x' - x) \delta(y' - y). \tag{11}$$

It is interesting to note that (9) can be rewritten as

$$f_1(x' - x, y' - y) = f(x' - x, y' - y) + \beta(x, y) n(x' - x, y' - y) \tag{12}$$

with

$$\beta(x, y) = 1 - \alpha(x, y)$$

giving for (11)

$$h_1(x', x, y', y) = h(x' - x, y' - y) + \beta(x, y) \cdot [\delta(x' - x) \delta(y' - y) - h(x' - x, y' - y)]. \tag{13}$$

Thus, their model can be seen as a linear combination of a stationary low-pass image and a nonstationary high-pass component. It therefore has a direct relation to various two-component image source models currently being used in image coding [12]-[14] and also to the earlier work of Schreiber [15] and Graham [16].

Its relationship to the structure of the visual system is equally direct. A large body of evidence now exists on the physiology of the retina [20]-[22], supporting the hypothesis that gradient detection plays an important part in the early stages of vision. This work is complemented by a number of psychophysical studies [23]-[25] showing a bandpass characteristic that can be explained in terms of spatial differentiation, or lateral inhibition [25]. Since this is a major function of the lower levels of the visual system, it is no surprise to find that conventional Wiener filters do not produce acceptable results. On the other hand, noise in "flat" regions of the image will excite these retinal detectors, giving rise to spurious features or textures. In regions where the gradient is large, however, the noise will have little effect, provided its variance is not sufficient to cause errors in detection. Thus, the weighting function $\beta(x, y)$ provides a compromise between resolution of genuine features and removal of those induced by the noise.

In seeking to improve this scheme, it is natural to examine the processing carried out by the higher levels of the visual system. The first important change in processing occurs in the visual cortex: cells are found which are selectively excited by

lines and edges of specific orientations. The studies of Hubel and Wiesel [26]-[28] have shown that an area in the primary cortex, area 17, consists of a regular array of linear feature detectors, each tuned to a line or edge of one orientation in a particular subfield of the field of vision. Daugman has discussed the Fourier domain properties such detectors are likely to have [34] and has shown the advantage of choosing functions which are separable in polar coordinates. The psychophysical studies of Kulikowski and King-Smith [29], [33] and Mostafavi and Sakrison [32] provide further evidence for the presence of anisotropic detectors. The latter work also suggests that detection may be incoherent, a hypothesis which some authors have advanced to explain the contradictory results which have been obtained on the bandwidth of the detectors [30], [31], [33]. These properties of the system lead to the conclusion that noise in the vicinity of a linear feature has an effect which depends on its orientation relative to the feature: noise in the same orientation may enhance detectability, but noise in the perpendicular direction will reduce it. This is confirmed by comparison of the images in Fig. 2. Both images were produced by anisotropic filtering of white noise in directions which depend on those of the linear features in the image of the face in Fig. 1. In the image on the left, the filter was aligned in the same direction as the lines and edges of Fig. 1; the image on the right was produced by aligning it at 90° to those directions. The structure of a face is clearly visible in the left image, but not in the right. Thus, local anisotropy is an important property of images, which should be incorporated into the estimator of (10) and (13).

Suppose, therefore, that $\varphi(x, y)$ defines at the point (x, y) the orientation in the Fourier domain of a local anisotropy. Then, expressing the spectra in polar Fourier coordinates ρ and θ

$$S_{f_1 f_1}(\rho) = S_{ff}(\rho) + \beta(x, y) S_{nn}(\rho) \tag{14}$$

the weighting function $\beta(x, y)$ should be modified by introducing a function of θ which is a maximum in the direction $\varphi(x, y)$ and falls to zero at $\varphi(x, y) \pm (\pi/2)$. An obvious choice of function which also has ideal interpolation properties (cf. Section IV) is $\cos^2(\cdot)$, giving in place of (14)

$$S_{f_2 f_2}(\rho, \theta) = S_{ff}(\rho) + \beta(x, y) \cos^2 [\varphi(x, y) - \theta] S_{nn}(\rho). \tag{15}$$

This results in an anisotropic filter $H_2(\cdot, \cdot, \cdot, \cdot)$

$$\begin{aligned} H_2(\rho, \theta, x, y) &= \frac{S_{ff}(\rho)}{S_{ff}(\rho) + {\sigma_n}^2} \\ &\quad + \beta(x, y) \frac{\cos^2 [\varphi(x, y) - \theta] {\sigma_n}^2}{S_{ff}(\rho) + {\sigma_n}^2} \\ &= H_i(\rho) + \beta(x, y) H_a(\rho, \theta, \varphi(x, y)). \end{aligned} \tag{16}$$

The filter of (15) represents an optimal solution for an image composed of a stationary isotropic component and a nonstationary, linear component. However, natural objects are curved: the "linearity" assumption is valid only locally and only if the curvature of objects is low. In other words, (15) applies only if the local rate of change of $\varphi(x, y)$ is small. If the average rate of change in an area is large, the effect of applying the filter $H_2(\cdot, \cdot, \cdot, \cdot)$ is similar to low-pass filtering, due to its low angular bandwidth.

Fig. 1. Image of face.

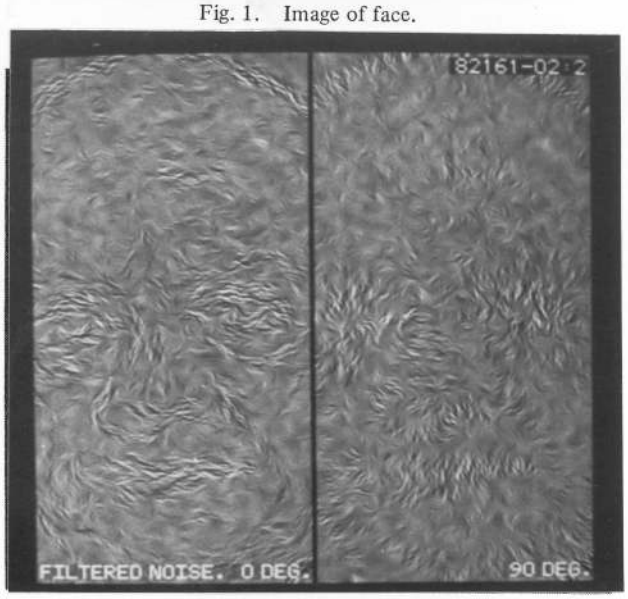

Fig. 2. White noise filtered at 0° (left) and 90° (right) to directions of edges in Fig. 1.

This problem can be solved if a function $\gamma(x, y)$, which provides a measure of local rate of change of angle, is available. In that case, it is possible to control the extent to which the local "equivalent signal" is isotropic and of high bandwidth, giving for (15)

$$\begin{aligned} S_{f_3 f_3}(\rho, \theta) &= S_{ff}(\rho) + \beta(x, y)[1 - \gamma(x, y)] \\ &\quad \cdot \cos^2 [\varphi(x, y) - \theta] S_{nn}(\rho) \\ &\quad + \beta(x, y) \gamma(x, y) S_{nn}(\rho). \end{aligned} \tag{17}$$

The result is a filter $H_3(\cdot, \cdot, \cdot, \cdot)$

$$\begin{aligned} H_3(\rho, \theta, x, y) &= H_i(\rho) + \beta(x, y)[1 - \gamma(x, y)] \\ &\quad \cdot H_a(\rho, \theta, \varphi(x, y)) \\ &\quad + \beta(x, y) \gamma(x\ y) H_i'(\rho) \end{aligned} \tag{18}$$

where $H_i(\cdot)$ and $H_a(\cdot)$ are as in (16) and

$$H_i'(\rho) = \frac{{\sigma_n}^2}{S_{ff}(\rho) + {\sigma_n}^2}. \tag{19}$$

The optimal filter thus consists of three parts, the first and third of which resemble the original solution of Abramatic and Silverman, with a middle term which is anisotropic. The information controlling the filters $H_a(\cdot, \cdot, \cdot)$ and $H_i'(\cdot)$ of (18) defines two images, known respectively as the first and second bias images.

III. ESTIMATION OF THE BIAS IMAGE

In the above derivation, it was assumed that the weighting functions $\beta(x, y)$ and $\gamma(x, y)$ and direction $\varphi(x, y)$ were known for each point in the image. It is of prime importance, therefore, to have an effective means for their estimation from the data $g(x, y)$. Note that the first bias image is complex (magnitude and direction) while the second is scalar.

At present, no truly optimal estimators are known for the bias images. Those that have been used experimentally are based on heuristic arguments and on ease of computation. What is required is to translate the rather vague title of "linear feature detectors" into an operational definition. An appreciation of the problem can be gained by considering the transforms of the ideal line $l(x, y)$ and edge $e(x, y)$

$$l(x, y) = \delta(x)/2\pi \quad e(x, y) = U(x)/2\pi$$

$$L(w_1, w_2) = \delta(w_2) \quad E(w_1, w_2) = \left(\pi\delta(w_1) + \frac{1}{jw_1}\right)\delta(w_2). \tag{20}$$

Thus, in the ideal case, energy in the transform domain is concentrated in an angle perpendicular to that in the spatial domain. This suggests a set of detectors whose bandwidths are high radially and low in angle. In order to encompass both types of feature, symmetric and antisymmetric functions are required.

Lines and edges are characterized by high gradient; the two-dimensional isotropic differential operator is the Laplacian [17]. A stationary, isotropic estimate of the image gradient with minimum mse is therefore found by convolving the Laplacian with the isotropic filter of (18), giving in the frequency domain

$$H_\nabla(\rho) = \rho^2 H_i(\rho). \tag{21a}$$

A directional estimate may be formed by weighting $H_\nabla(\cdot)$ with a suitable angular function $w(\cdot)$, say. To remove phase dependence from the estimate, a pair of quadrature filters must be used, giving a line filter $H_l(\cdot, \cdot)$ and edge filters $H_e(\cdot, \cdot)$

$$H_l(\rho, \theta) = w(\theta) H_\nabla(\rho) \tag{21b}$$

$$H_e(\rho, \theta) = j \operatorname{sgn}(\cos\theta) H_l(\rho, r). \tag{21c}$$

The filters oriented in the kth of N directions are then

$$H_l^k(\rho, \theta) = H_l(\rho, \theta - \theta_k)$$

$$H_e^k(\rho, \theta) = H_e(\rho, \theta - \theta_k). \tag{22}$$

The direction and magnitude of the bias are not, however, simply related to the outputs of these filters. Since computational limitations dictate a small value of N, typically 4, some form of interpolation is required in estimation of the angle. Measurement of the magnitude also poses a problem, since when the local field is wide-band and isotropic, all the outputs will be large.

For $N = 4$, both problems can be solved by appropriate choice of the weighting function $w(\cdot)$

$$w(\theta) = \cos^2\theta. \tag{23}$$

Then define $E_k(\cdot, \cdot)$ by

$$E_k(x, y) = \sqrt{{S_k}^2(x, y) + {C_k}^2(x, y)} \tag{24}$$

with

$$S_k(x, y) = h_e^k(x, y) * g(x, y)$$

$$C_k(x, y) = h_l^k(x, y) * g(x, y)$$

and

$$V(x, y) = \sum_{k=1}^{4} E_k(x, y)/V_m. \tag{25}$$

Define $D(x, y)$ by

$$D(x, y) = \sqrt{[E_1(x,y) - E_3(x,y)]^2 + [E_2(x,y) - E_4(x,y)]^2}/D_m. \tag{26}$$

V_m and D_m are normalizing constants. The angle $\varphi(x, y)$ is found from

$$\sin 2\varphi(x, y) = [E_2(x, y) - E_4(x, y)]/D(x, y)$$

$$\cos 2\varphi(x, y) = [E_1(x, y) - E_3(x, y)]/D(x, y). \tag{27}$$

The estimate of $\varphi(x, y)$ is expressed in the form of (27) to avoid the degeneracy associated with the inverse trigonometric functions. It is simple to show that when the neighborhood of the point (x, y) contains a one-dimensional field (e.g., straight line or edge) at an angle θ, these formulas give the correct value of θ (see Fig. 3).

Averaging of $V(x, y)$ with an isotropic smoothing function $h_s(\cdot, \cdot)$ produces a measure $B_h(x, y)$ of the local high-pass energy

$$B_h(x, y) = h_s(x, y) * V(x, y). \tag{28a}$$

Smoothing of the vector field defined by $D(x, y)$ and $\varphi(x,$

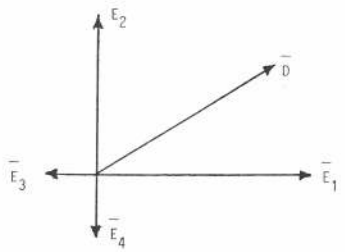

Fig. 3. Bias direction produced by vector addition of outputs from four directional filters.

y) gives a measure $B_a(x, y)$ of local one-dimensional energy

$$B_a(x, y)) = \| h_s(x, y) * \bar{D}(x, y)) \|. \tag{28b}$$

The control information $\beta(x, y)$ and $\gamma(x, y)$ can then be written as

$$\beta(x, y) = |B_h(x, y)|^{\epsilon} \qquad 0 \leqslant \epsilon \leqslant 1$$

$$\gamma(x, y) = 1 - B_a(x, y)/B_h(x, y). \tag{29}$$

Thus, $\beta(x, y)$ is a direction insensitive estimate of the relative nonstationarity in the neighborhood of (x, y) and $\gamma(x, y)$ measures the variability in angle. The exponent ϵ controls the extent to which the estimate depends on relative or absolute magnitude. In the coding experiments, a thresholded version of $\gamma(x, y)$ was used, with little obvious degradation in performance.

IV. A SUBOPTIMAL IMPLEMENTATION

The major problem with the estimators described above is the computational one. Even when a dedicated, high-speed processor of the type described in [37] is available, the sheer volume of computation on a $(512)^2$ image imposes a constraint on the size of the filter masks which can be employed.

For this reason, the filters are spatially limited to a square array of $(15)^2$ elements. This imposes certain restrictions on the allowable shape of the filters: they must be of smooth variation in the frequency domain if a reasonable finite impulse response approximation is to be obtained. In order to overcome this problem, filter functions with the desired properties have been selected and a least-squares optimization procedure used to derive the spatial masks [36].

The isotropic filter $H_i(\cdot)$ of (16) is given by

$$H_i(\rho) = \begin{cases} \cos^2\left(\dfrac{\pi\rho}{1.8}\right) & \rho \leqslant 0.9 \\ 0 & \rho > 0.9. \end{cases} \tag{30}$$

The anisotropic filter $H_a(\cdot, \cdot, \cdot)$ is

$$H_a(\rho, \theta, \varphi) = H_a(\rho) H_a(\theta, \varphi) \tag{31}$$

with

$$H_a(\rho) = \begin{cases} 1 - H_i(\rho) & \rho \leqslant 0.9 \\ 1 & 0.9 < \rho \leqslant \pi - 0.9 \\ \cos^2 \dfrac{\pi}{1.8} (\rho - \pi + 0.9) & \pi - 0.9 < \rho \leqslant \pi \end{cases} \tag{32}$$

$$H_a(\theta, \varphi) = \tfrac{1}{2} [1 + \cos \varphi H_c(\theta) + \sin \varphi H_s(\theta)]$$

$$H_c(\theta) = \cos \theta$$

$$H_s(\theta) = \sin \theta.$$

Note that because of the ideal interpolation properties of the trigonometric functions, the anisotropic filter in any direction can be obtained by interpolation from only three fixed filters.

In (32) π radians corresponds to the maximum image frequency (0.5 cycle/pixel). These functions are illustrated in Fig. 4. Once again, the choice of (33) for the angular dependence of $H_a(\cdot)$ was dictated by the need for interpolation. The same considerations led to the following choice of line and edge detectors $H_e(\cdot, \cdot)$ and $H_l(\cdot, \cdot)$

$$H_e(\rho, \theta) = H_e(\rho) H_e(\theta) \tag{34}$$

$$H_l(\rho, \theta) = H_e(\rho) H_l(\theta) \tag{35}$$

$$H_e(\rho) = \exp - \left[\frac{4 \ln 2}{\ln^2 B} \ln^2 (\rho/\rho_c) \right] \tag{36}$$

$$H_l(\theta) = \cos^2 \theta \tag{37}$$

$$H_e(\theta) = j H_l(\theta) \operatorname{sgn} (\cos \theta). \tag{38}$$

Unlike the optimal filters, these functions are not dependent on signal-to-noise ratio. In order to provide some measure of adaptability in this respect, it has been found useful to reduce the bandwidth of the isotropic filter, $h_s(\cdot)$ [see (28)], when the signal-to-noise ratio is low. Similarly, it has proved advantageous in such circumstances to perform several iterations of the enhancement process. This can be represented by

$$\hat{f}^n(x, y) = \hat{f}^{n-1}(x' - x, y' - y) * h_3(x' - x, y' - y) \quad n > 1$$

$$\hat{f}^1(x, y) = g(x, y). \tag{39}$$

This has the effect of increasing the rolloff rate of the filters in a way similar to that which would be obtained in the optimal solution (18).

V. APPLICATION TO IMAGE RESTORATION

Experiments have been performed to test the utility of the estimator in the restoration of images corrupted by additive white Gaussian noise. It has also been used in the pre- and postprocessing of images coded by the predictive coder described in Part II of the paper (cf. Part II, Section V).

The first experiment was designed to test the filters on a "noise-free" image. The results of this test are shown in Figs. 5-8. The original image is shown in Fig. 5 and its associated control images in Figs. 7 and 8. Examination of Figs. 7 and 8 show how the control information $\beta(x, y)$, $\varphi(x, y)$, and $\gamma(x, y)$ affects the estimate. Note that $\gamma(x, y)$ is nonzero only in highly curved regions (e.g., around the eyes) and in complex areas, such as the feathers on the hat. In these regions, therefore, the estimate is isotropic. In Fig. 6, the effects of two iterations of the filtering algorithm can be seen. Two properties of the filtered image are immediately apparent: in areas of smooth variation it appears less noisy than the original; its

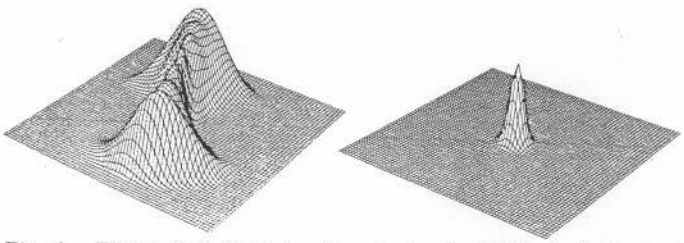

Fig. 4. Filters used in restoration: isotropic (right); (anisotropic + isotropic) (left).

Fig. 5. Original image of face.

Fig. 6. Enhancement of Fig. 5 (two iterations).

Fig. 7. First bias image from Fig. 5.

Fig. 8. Second bias image from Fig. 5.

edges have been enhanced. A closer study reveals the presence of Mach bands at the edges. The overall result is an image which many observers prefer to the original. The observed effects have an obvious relation to the structure of the filter: low-pass isotropic filtering of areas of smooth variation increases the signal-to-noise ratio therein; directional filtering in the anisotropic regions removes the more visible noise components and can (with appropriate weighting functions) emphasize both edges and lines. That the result should be pleasing to human viewers is confirmation of the importance they attach to these features.

When noise is added to the image, similar results are obtainable, provided the signal-to-noise ratio is not too low. Figs. 9-11 show the effect of filtering an image containing white noise with a variance which was 10 percent of the signal variance. The bias image of Fig. 10 was estimated from the noisy data (Fig. 9) and two iterations of filtering performed to give the image of Fig. 11. Under these conditions, there is virtually no difference between the enhanced image and that obtained before (Fig. 6). When the signal-to-noise ratio is reduced still further, a degradation in performance is inevita-

Fig. 9. Image of Fig. 5 plus white noise (10 dB S/N).

Fig. 10. Bias image taken from Fig. 9.

Fig. 11. Restoration of Fig. 9 (four iterations).

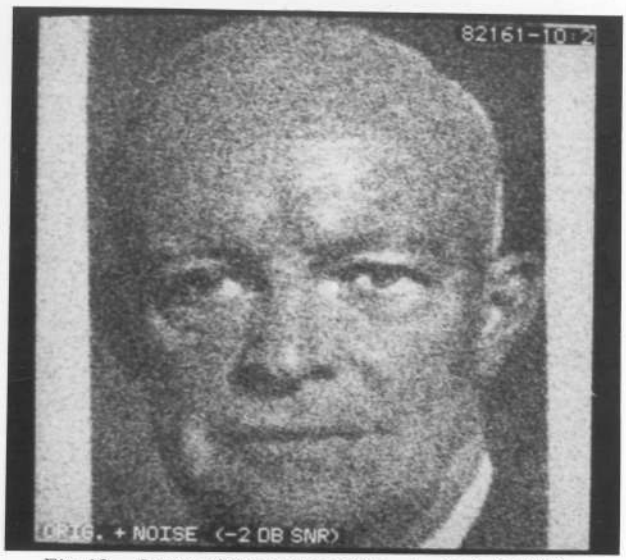

Fig. 12. Image of Fig. 1 plus white noise (−2 dB S/N).

Fig. 13. Bias image taken from Fig. 1.

ble. Figs. 12-16 show that this is largely due to the difficulty in estimating the bias image. Fig. 12 shows the image of Fig. 1 corrupted by noise whose variance is approximately equal to that of the signal (−2 dB S/N ratio). Figs. 15 and 16 show the effect of four iterations with the filter using bias images taken from the original (Fig. 13) and noisy pictures (Fig. 14), respectively. Note that in this case, the complexity measure $\gamma(x, y)$ is of no utility because there is too much noise present. The estimate in this case is obtained by setting $\gamma(x, y) = 0$ everywhere. The loss of resolution in the bias and noise introduced in low-pass areas of the image show their effects clearly in this case: genuine features are weakened and spurious ones introduced. In spite of this, there is still a definite improvement in image quality.

While images such as those above constitute an important class of image, they can hardly be described as representative of images in general. In particular, neither image contains much texture. In order to investigate its effect on textures, the algorithm has been used on two quite different images—a fingerprint (Fig. 17) and a landscape containing trees and a lake (Figs. 18-21). Fig. 17 demonstrates the utility of the

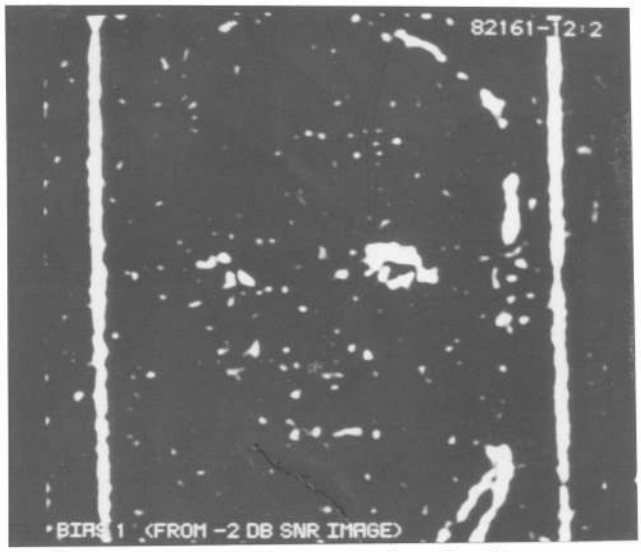

Fig. 14. Bias image taken from Fig. 12.

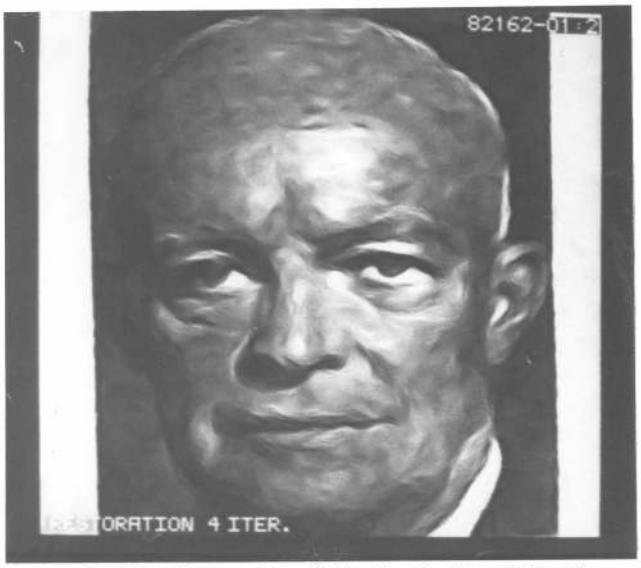

Fig. 15. Restoration of Fig. 12 using bias of Fig. 13.

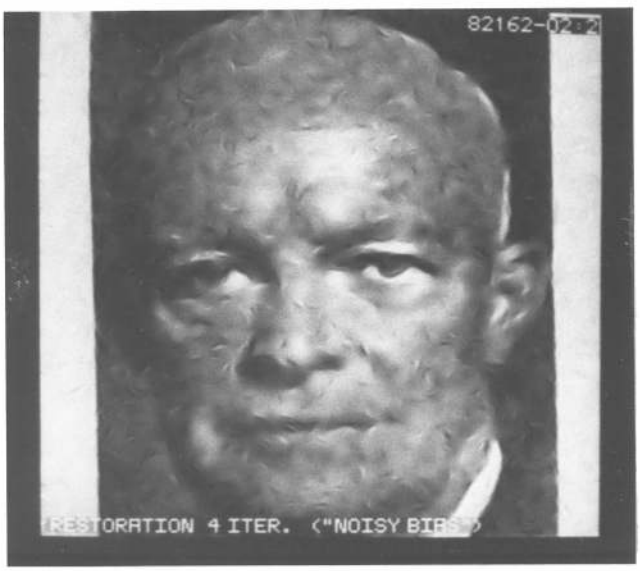

Fig. 16. Restoration of Fig. 12 using bias of Fig. 14.

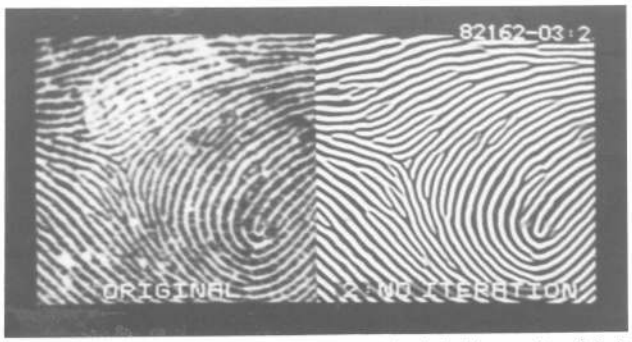

Fig. 17. Restoration of fingerprint: original (left); result of 2 iterations (right).

Fig. 18. Original landscape.

Fig. 19. Effect of enhancement operations on Fig. 18.

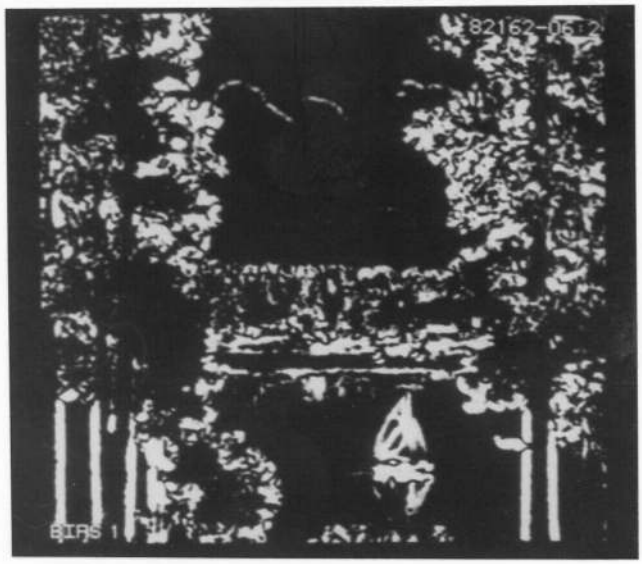

Fig. 20. First bias image from Fig. 18.

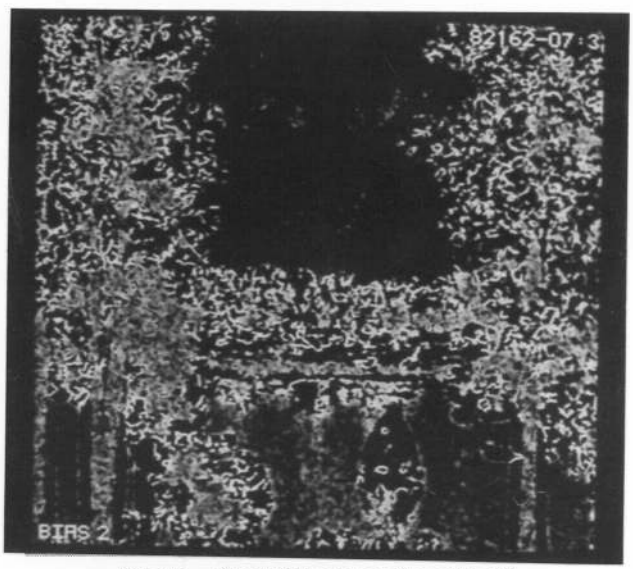

Fig. 21. Second bias image from Fig. 18.

algorithm in the "cleaning-up" of a fingerprint, the original of which was very noisy. Thus, in cases where the texture is coarse relative to the filter dimensions, the algorithms works well. In the converse case, such a result could hardly be expected. The fine structure of the foliage in the landscape image is almost completely removed by filtering, as is apparent from a comparison of Figs. 18 and 19. The control images (Figs. 20 and 21) give the reason for this: the filters used in estimation of the bias have too low a bandwidth to provide an adequate representation of fine structure. While this effect is noticeable, it does not seem as objectionable as that produced by simple low-pass filtering of the image. This suggests that fine textures are of relatively minor importance in vision.

Taken together, the results show precisely those qualities of the estimator which could be anticipated from its structure: smoothing of low-pass regions, enhancement of edges, and some loss of fine texture. More important, their combined effect is images which are more acceptable than those obtained using conventional techniques.

VI. CONCLUSIONS

An anisotropic nonstationary estimator, based on the "signal equivalent" approach, has been shown to be optimal for the class of images which contain significant line and edge features. The relation of this model to the behavior of the visual system has been described. It has been shown that a computationally feasible suboptimal approach is capable of producing acceptable results from images corrupted by white noise. A method of estimating the nonstationary control information has been described and was shown to be effective except when the noise level is high.

While these results are encouraging, it is evident that to gain a more general applicability, certain problems must be resolved. In particular, the procedure used to estimate the bias image is capable of refinement. A scheme which is more nearly optimal is required when the signal-to-noise ratio in the data is low. Furthermore, some means of incorporating a fine texture description into the scheme must be found. It is unfortunate that these two requirements are to a certain extent contradictory, since fine textures are more than a little "noise-like" in appearance. In general, there seems no simple way of recognizing, for a given image, when fine texture is due to noise and when it is a genuine image property. Only by a recourse to a more global description of the image can such a question be answered. However, one of the features of the "general operator" approach is precisely that it leads to a hierarchical processing structure [19], [35]. Investigations are currently under way to see if these ideas can provide the means for solution of this problem.

With the incorporation of such improvements, the estimator should have wide applicability. As it is at present, it should prove useful in a number of areas, not simply for enhancement, but also as a preprocessor for coding and pattern recognition tasks, since the methods employed are often particularly sensitive to noise. Furthermore, the methods described in Section II suggest a new form of distortion measure [39]. It is hoped to present results in this area soon.

ACKNOWLEDGMENT

The authors would like to thank members of the GOP group for their help in the project.

REFERENCES

[1] C. W. Helstrom, "Image restoration by the method of least squares," *J. Opt. Soc. Amer.*, vol. 57, no. 3, pp. 297–303, 1967.
[2] W. K. Pratt, "Generalized Wiener filtering computation techniques," *IEEE Trans. Comput.*, vol. C-21, pp. 297–303, July 1972.
[3] B. R. Hunt, "The application of constrained least squares estimation to image restoration by digital computer," *IEEE Trans. Comput.*, vol. C-22, pp. 805–812, 1973.
[4] G. L. Anderson and A. N. Netravali, "Image restoration based on a subjective criterion," *IEEE Trans. Syst., Man, Cybern.*, vol. SMC-6, pp. 845–853, Dec. 1976.
[5] V. K. Ingle and J. W. Woods, "Multiple model recursive estimation of images," in *Proc. IEEE Conf. Acoust., Speech, Signal Processing*, Washington, DC, 1979, pp. 642–645.
[6] J. F. Abramatic and L. M. Silverman, "Non-stationary linear restoration of noisy images," in *Proc. IEEE Conf. Decision Contr.*, Ft. Lauderdale, FL, 1979, pp. 92–99.
[7] H. Knutsson, R. Wilson, and G. H. Granlund, "Anisotropic filter-

ing operations for image enhancement and their relation to the visual system," in *Proc. IEEE Conf. Pattern Recognition, Image Processing*, Dallas, TX, 1981.
[8] C. C. Cutler, "Differential quantization of communication signals," U.S. Patent 2 605 361, 1952.
[9] J. B. O'Neal, Jr., "Predictive quantising systems (differential pulse code modulation) for the transmission of television signals," *Bell Syst. Tech. J.*, vol. 45, pp. 689–721, 1966.
[10] J. C. Candy and R. H. Bosworth, "Methods for designing differential quantizers based on subjective evaluations of edge busyness," *Bell Syst. Tech. J.*, vol. 51, no. 7, pp. 1495–1516, 1972.
[11] A. Habibi, "Survey of adaptive image coding techniques," *IEEE Trans. Commun.*, vol. COM-25, pp. 1275–1284, 1977.
[12] J. K. Yan and D. J. Sakrison, "Encoding of images based on a two-component source model," *IEEE Trans. Commun.*, vol. COM-25, pp. 1315–1322, 1977.
[13] D. Anastassiou and D. J. Sakrison, "New bounds to $R(D)$ for additive sources and applications to image coding," *IEEE Trans. Inform. Theory*, vol. IT-25, no. 2, pp. 145–155, 1979.
[14] A. K. Jain, "Image data compression: A review," *Proc IEEE*, vol. 69, pp. 349–389, Mar. 1981.
[15] W. F. Schreiber, C. F. Knapp, and N. D. Kay, "Synthetic highs: An experimental TV bandwidth reduction system," *J. Soc. Motion Picture TV Eng.*, vol. 68, pp. 525–537, 1959.
[16] D. N. Graham, "Image transmission by two-dimensional contour coding," *Proc. IEEE*, vol. 55, pp. 336–346, 1967.
[17] A. Rosenfeld, *Picture Processing by Computer*. New York: Academic, 1969.
[18] W. Frei and C. C. Chen, "Fast boundary detection: A generalization and a new algorithm," *IEEE Trans. Comput.*, vol. C-26, pp. 988–998, 1977.
[19] G. H. Granlund, "In search of a general picture processing operator," *Comput. Graphics, Image Processing*, vol. 8, no. 2, pp. 155–173, 1978.
[20] C. Enroth-Cugell and J. G. Robson, "The contrast sensitivity of retinal ganglion cells of the cat," *J. Physiol.*, vol. 187, pp. 517–552, 1966.
[21] B. G. Cleland and W. R. Levick, "Brisk and sluggish concentrically organised ganglion cells in the cat's retina," *J. Physiol.*, vol. 240, pp. 421–456, 1974.
[22] L. N. Thibos and F. S. Werblin, "The response properties of the steady antagonistic surround in the mudpuppy retina," *J. Physiol.*, vol. 278, pp. 79–99, 1978.
[23] F. W. Campbell and J. G. Robson, "Application of Fourier analysis to the visibility of gratings," *J. Physiol.*, vol. 197, pp. 551–566, 1968.
[24] H. R. Wilson and J. R. Bergen, "A four mechanism model for threshold spatial vision," *Vision Res.*, vol. 19, pp. 19–32, 1979.
[25] D. H. Kelly, "Spatial frequency selectivity in the retina," *Vision Res.*, vol. 15, pp. 565–572, 1975.
[26] D. H. Hubel and T. N. Wiesel, "Receptive fields of single neurones in the cat's striate cortex," *J. Physiol.*, vol. 148, pp. 574–591, 1959.
[27] ——, "Receptive fields, binocular interaction and functional architecture in the cat's visual cortex," *J. Physiol.*, vol. 160, pp. 106–154, 1962.
[28] ——, "Brain mechanisms of vision," *Sci. Amer.*, Sept. 1979.
[29] J. J. Kulikowski and P. E. King-Smith, "Spatial arrangement of line, edge and grating detectors revealed by subthreshold summation," *Vision Res.*, vol. 13, pp. 1455–1478, 1973.
[30] C. F. Stromeyer and S. Klein, "Spatial frequency channels in human vision as asymmetric (edge) mechanisms," *Vision Res.*, vol. 14, pp. 1409–1420, 1974.
[31] G. E. Legge, "Space domain properties of a spatial frequency channel in human vision," *Vision Res.*, vol. 18, pp. 959–969, 1978.
[32] H. Mostafavi and D. J. Sakrison, "Structure and properties of a single channel in the human visual system," *Vision Res.*, vol. 16, pp. 957–968, 1976.
[33] P. E. King-Smith and J. J. Kulikowski, "The detection and recognition of two lines," *Vision Res.*, vol. 21, pp. 235–250, 1981.
[34] J. G. Daugman, "Two-dimensional analysis of cortical receptive field profiles," *Vision Res.*, vol. 20, pp. 447–456, 1980.
[35] G. H. Granlund, "Description of texture using the general operator approach," in *Proc. IEEE Conf. Pattern Recognition*, Miami, FL, 1980.
[36] H. Knutsson and G. H. Granlund, "Fourier domain in design of line and edge detectors," in *Proc. IEEE Conf. Pattern Recognition*, Miami, FL, 1980.
[37] K. Lundgren, D. Antonsson, and G. H. Granlund, "GOP, a different architecture for fast and flexible image processing," in *Proc. Nat. Comput. Conf.*, Chicago, IL, 1981.
[38] A. Papoulis, *Probability, Random Variables and Stochastic Processes*. New York: McGraw-Hill, 1965.
[39] G. H. Granlund, "A non-linear, image content dependent measure of image quality," Linkoeping Univ., Linkoeping, Sweden, Internal Rep. LiTH-15Y-0189, 1977.

★

Hans E. Knutsson was born in Jaemtland, Sweden, on December 17, 1950. He received the M.S. degree in electrical engineering from Linkoeping University, Linkoeping, Sweden, in 1975. He is currently working toward the Ph.D. degree in computer science at Linkoeping University.

He is currently a Research Assistant at the Picture Processing Laboratory, Department of Electrical Engineering, Linkoeping University. His research interests are in image analysis and image understanding, in particular, questions concerning image information representation and hierarchical structures for information processing.

★

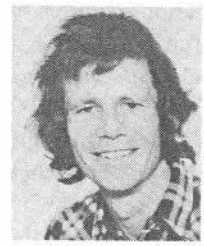

Roland Wilson was born in Hertford, England, on March 18, 1949. He received the B.Sc. degree in electronics and the Ph.D. degree from the University of Glasgow, Glasgow, Scotland, in 1971 and 1978, respectively.

In 1971–1972 he was with STL Laboratories, Harlow, England. In 1978 he joined the University of Aston, Birmingham, England, as a Lecturer. He has worked in the fields of television picture transmission and physiological system identification. His current interests include aspects of information theory and picture processing. At present he is on study leave at the Picture Processing Laboratory, Linkoeping University, Linkoeping, Sweden.

★

Goesta H. Granlund (S'66–M'66–M'79) began working in 1966 with SAAB-SCANIA Electronics Division, Sweden, on computer systems and control systems. In 1970 he came to the Massachusetts Institute of Technology, Cambridge, first as a Postdoctoral Fellow and later as a member of the Research Staff, where he worked on biomedical pattern recognition and, in particular, systems for automated analysis and recognition of chromosomes. He is currently Professor of Electrical Engineering at Linkoeping University, Linkoeping, Sweden, where he has been since 1972, with one year as Visiting Professor at M.I.T. in 1974–1975. He has a Research Group in the Picture Processing Laboratory of Linkoeping University, working on various image processing problems such as reconstruction, image information representation, feedback and relaxation methods, and parallel processing structures. He has written more than 50 articles within the field of image processing and pattern recognition, and he has given international courses within this field. He has also been working as a consultant for several international companies in the field of image processing and pattern recognition.

Dr. Granlund is a member of several professional societies and he is President of the European Association for Signal Processing (EURASIP).